STUDIES OF NUCLEATION AND GROWTH, SPECIFIC HEAT AND VISCOSITY OF UNDERCOOLED MELTS OF QUASICRYSTAL AND POLYTETRAHEDRAL-PHASE FORMING ALLOYS

K. F. Kelton[1*], A. K. Gangopadhyay[1], G. W. Lee[1], R. W. Hyers[2], T. J. Rathz[3], M. B. Robinson[2], and J. Rogers[2]

Washington University, St. Louis, MO[1], NASA, Marshall Space Flight Center[2], University of Alabama, Huntsville, AL[3]

1. Introduction

Fahrenheit first recognized that many liquids can be maintained out of equilibrium (i.e. below the melting temperature) for long periods without crystallizing[1]. The amount of undercooling attainable before solidification is often quite large, up to one third of the melting temperature, as was observed for liquid mercury[2]. Such a dramatic undercooling for a liquid metal is surprising, given the similarity in the densities of metallic liquids and solids, and the similar average interatomic distances and coordination numbers. It is now recognized that all liquids can be deeply undercooled, typically to approximately 20% of their liquidus temperatures[3]. This resistance to crystallization indicates that a substantial barrier separates the initial and final states.

Frank first argued that this transformation barrier arises from different local atomic configurations in the liquid and the crystal[4]. The relatively weak non-covalent bonding in many metals leads to their tendency to crystallize into relatively close-packed structures, which can be usefully modeled by a packing of hard spheres. Face-centered-cubic (fcc) and close-packed hexagonal (cph) are the most densely packed periodic structures. However, an icosahedral packing, is even denser. For a pair-wise central potential, such as the Lennard-Jones potential, the fully relaxed energy of icosahedral packing is, therefore, lower than that of fcc or cph. While icosahedral packing is incompatible with translation periodicity, it might be a natural choice for liquid and amorphous phases. Crystallization would then require that the local icosahedral order be transformed to an allowed crystallographic one, costing energy. This may provide a natural barrier for nucleation of a crystalline phase from the liquid.

The stability of icosahedral clusters is evident in the "magic numbers" for the total atoms in free atomic clusters[5,6]. Further, the results of molecular dynamics simulations and some physical property measurements are consistent with this presumed icosahedral order in liquids. However, it has not been observed directly. Quasicrystals, a new class of condensed matter discovered by Shechtman and co-workers in 1984 [7], have extended icosahedral order. A low interfacial energy for the nucleation of quasicrystals from liquids and glasses[8] is consistent with the existence of similar order in the liquid.

Measurements of the maximum undercooling and growth velocity of undercooled liquids that form quasicrystals and related crystal approximant phases can allow a study of the nucleation and growth mechanisms for complex periodic and ordered nonperiodic phases. Further, since quasicrystals generally

have a composition different from that of the initial liquid phase, undercooling studies allow an investigation of nucleation processes when the composition of the initial and final phases are different. Quantitative measurements of the melt viscosity and specific heat as a function of alloy composition near the ideal stoichiometry of the phases with icosahedral order can be used to investigate the onset of icosahedral order in undercooled liquids. Undercooling and thermo-physical property measurements can, then, lead to a deeper understanding of the structure of the undercooled liquids, and better inform us of processes that are central in all materials development and production.

Ti-Zr-Ni alloys are particularly well suited for such experiments. Over the past decade this research group has identified many interesting phases in this alloy system. Three that are most relevant for the research under this grant are, a) β-Ti/Zr (bcc) solid solution, b) C14 Laves phase, and c) a stable icosahedral (i-phase) phase. The complexity of the local structure of these phases increases in the order listed above, providing a unique opportunity to study nucleation as a function of increasing polytetrahedral order in the same alloy system. Containerless processing with the electrostatic levitation (ESL) facility at the Marshall Space Flight Center (MSFC), Huntsville, Al, has not only allowed us to study the undercooling behavior of these alloys as a function of composition, but also to make thermo-physical property measurements in the liquid and undercooled state. In addition, the beamline ESL (BESL) facility, recently developed to measure in-situ structural properties using synchrotron radiation at the Advanced Photon Source (APS, MU-CAT) at Argonne National laboratory, has allowed us to make the first studies of the developing icosahedral order in the liquid as a function of undercooling. These ground-based studies have demonstrated the feasibility and need to conduct benchmark nucleation experiments on the International Space Station (ISS). Those results are discussed briefly here.

2. Phase Diagram Determination of Ti-Zr-Ni Alloys
A quantitative analysis of undercooling data requires that the phase diagram be known near the alloy compositions of interest. To investigate this, we have made an exhaustive study of the phase microstructures in as-cast and annealed samples. As-cast ingots (0.5 g) of Ti-Zr-Ni were prepared over a wide composition range ($Ti_{(25-65)}Zr_{(20-54)}Ni_{(2-40)}$) from high-purity elements Ti (99.995%), Zr (99.9%) and Ni (99.995). The as-cast alloys were annealed at various temperatures (500 °C < T < 850 °C) for various lengths of times. Using x-ray powder diffraction, and scanning and transmission electron microscopy, equipped with energy dispersive x-ray spectroscopy, the equilibrium phases in the as-cast and annealed samples at various temperatures were identified and quantified. Because conventional techniques (DTA, DSC, etc.) are unreliable for highly reactive high melting point alloys, ESL studies were used to determine the solidus and liquidus temperatures of these alloys. A cut of the Ti-Zr-Ni phase diagram for equal Ti and Zr concentrations, constructed from these extensive studies, is shown in Fig. 1 as an illustration. For low Ni (≤ 5 at.%) concentrations, β-Ti/Zr (bcc, with a = 3.43 Å at 700 °C[9]) is the primary solidification phase from the liquid. As the temperature decreases, β(Ti/Zr) undergoes an allotropic transformation (*i.e.* a structural transformation with no change in composition) to α(Ti/Zr) (hcp, a = 3.12 Å, c = 4.94 Å) in the temperature range of 550 – 650 °C (depending on the Ti/Zr ratio). With increasing Ni, the liquidus temperature decreases and the alloy becomes a mixture of β(Ti/Zr) and the C14 Laves phase (a polytetrahedral hcp phase with a = 5.22 Å and c = 8.56 Å). Due to the allotropic transformation, the as-cast alloys, however, always contain α(Ti/Zr) instead of β(Ti/Zr).
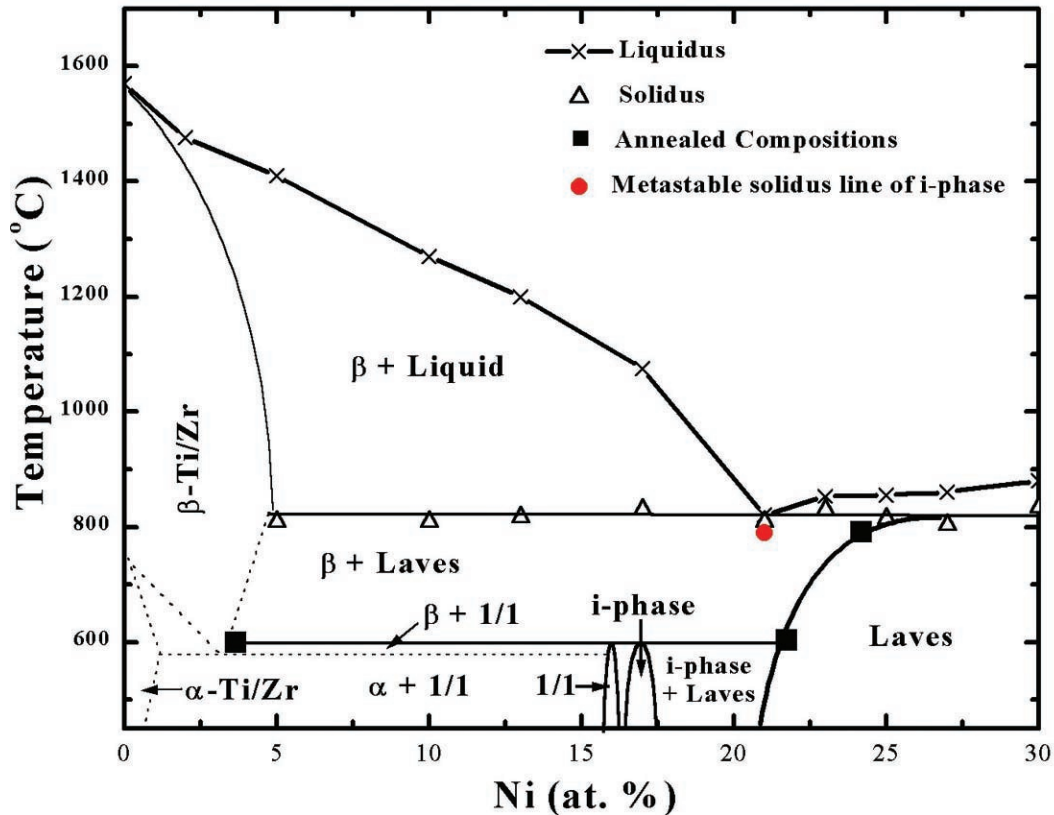
Fig. 1. Vertical section of the Ti-Zr-Ni phase diagram for a Ti/Z ratio equal to one. The symbols are the experimental data and the solid and dashed lines indicate the phase boundaries.

For alloys made with 16-18 at.% Ni, the stable phase for T < 570 °C is, surprisingly, not a mixture of α(Ti/Zr) and the C14 Laves phase. Extensive annealing studies over this temperature and composition range show that the lowest temperature phase is either an icosahedral phase with a quasi-lattice constant of 5.21-5.24 Å, or the 1/1 crystal approximant (bcc, a = 14.32 Å). One of the important challenges of the ESL undercooling studies was to explore whether the i-phase may become the primary crystallizing phase from the undercooled liquid, if the nucleation of β(Ti/Zr) and the C14 Laves phases were avoided.

One interesting feature of the phase diagram is the existence of an eutectic phase around 21 at.% Ni composition. Below the eutectic temperature, $Ti_{39.5}Zr_{39.5}Ni_{21}$ should crystallize to a eutectic mixture of the β(Ti/Zr) and the C14 phase. As indicated by the filled circle in Fig. 1, recent studies[10] of rapidly solidified droplets at this composition, however, show a recalescence at 700 °C and a solidification plateau at approximately 790 °C, which correspond to the nucleation and growth of the icosahedral phase[10]. This temperature is only slightly below the eutectic temperature. As indicated in the vertical section, extensive investigations have shown that the i-phase is stable only at temperatures below 600°C; no alloy concentration has been found where the i-phase is stable at higher temperatures. As will be discussed soon, this $Ti_{39.5}Zr_{39.5}Ni_{21}$ i-phase is actually a metastable solidification product. Nevertheless, it is the primary solidification phase at the cooling rates found in ESL, allowing studies to be made of the nucleation kinetics for the Ti-Zr-Ni i-phase.

Above 25 at. % Ni, the primary crystallizing phase is the C14 Laves phase. The local atomic structure of this polytetrahedral periodic phase is presumed to be similar to that of the i-phase[11]. This provides

329

another opportunity to study the nucleation of a polytetrahedral phase, in addition to the i-phase, using the MSL-EML on the ISS.

3. Electrostastic Levitation (ESL) Studies
3.1 Undercooling Behavior
Based on the phase diagrams presented in §2 a large number of Ti-Zr-Ni alloys were selected for processing in the electrostatic levitator (ESL) at MSFC. ***The primary objective of these ESL studies was to identify the crystallizing phases that nucleate directly from the undercooled liquid, study their undercooling behavior, identify the compositions of most interest for studies using the MSL-EML facility planned for the ISS, and to understand the fundamental process of nucleation of polytetrahedral phase forming alloys***.

Fig. 2 shows the measured sample temperature as a function of time during free radiative cooling in the ESL for some representative Ti-Zr-Ni alloys. These are shown as a function of increasing Ni ($0 < \text{Ni} < 17$ at.%), but for equal Ti/Zr concentrations. A single recalescence event marks the nucleation and growth of β(Ti/Zr) for the alloy containing 2 at.% Ni (Fig. 2(a)). The small recalescence at approximately 550 °C is due to the β(Ti/Zr) to α(Ti/Zr) transformation. In contrast, the $Ti_{47.5}Zr_{47.5}Ni_5$ alloy shows an additional small plateau near 750 °C (see inset of Fig. 2(b)), signaling the formation of the C14 Laves phase from the remainder of the liquid. The volume fraction of this phase is very small, however, and is not evident in the x-ray diffraction patterns, but it is found in SEM studies of the solidification microstructure. The lower temperature recalescence is much more prominent in the 13 at.% and 17 at.% Ni samples, with a corresponding decrease in the high temperature event. This indicates a decrease in the crystalline volume fraction of the β(Ti/Zr) phase and an increase in the volume fraction of the C14 Laves phase as the Ni concentration is increased. These points were further confirmed by powder x-ray diffraction and SEM studies on the ESL processed samples and are consistent with the phase diagram (Fig. 1). The onset temperature of the high temperature recalescence (nucleation of the β(Ti/Zr) phase) decreases with increasing Ni, due to a decrease in the liquidus. The reduced undercooling of the β(Ti/Zr) phase ($\Delta T_r = (T_m - T_r)/T_m$) increases slightly from 0.16 to 0.20 with increasing Ni; a value typical for simple phase forming alloys.

Interestingly, for alloys containing about 21 at.% Ni (Fig. 3(a)), a two step recalescence is observed. The first plateau temperature is approximately 785 °C and the second plateau temperature, corresponding to the solidus temperature, is approximately 810 °C. The liquidus temperature is about 820 °C. The Ni concentration is critical for the occurrence of the step recalescence; the Ti/Zr concentration is less critical (occurring for 29 at.% $\leq$ Ti $\leq$ 45 at.%), however. Based on the phase diagram, the low temperature recalescence ***should*** correspond to the formation of the C14 Laves phase. The plateau temperature is, however, approximately 25 °C below the expected solidus temperature (810 °C). Were it due to the formation of β(Ti/Zr),
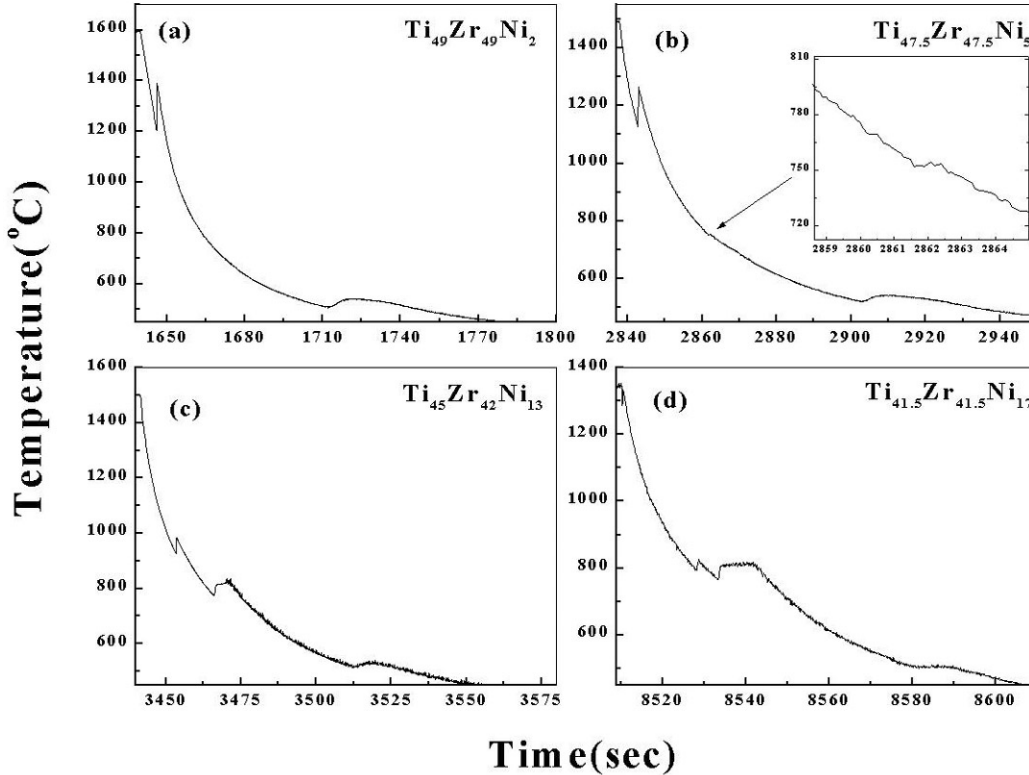
Fig. 2. Temperature-time cooling curves for Ti-Zr-Ni alloys.

the plateau temperature should be even higher. Further, the reduced undercooling for this alloy (≈ 0.12) is much smaller than is typically observed for the β(Ti/Zr) phase (0.18 on the average). Although the recalescence events are inconsistent with the nucleation of either the C14 Laves or the β(Ti/Zr) phase, the x-ray diffraction pattern or the SEM micrographs of these ESL processed alloys show a phase mixture of C14 Laves and the β(Ti/Zr) phase. This apparent contradiction was resolved by in-situ x-ray diffraction studies during recalescence in the beamline ESL (BESL), as will be demonstrated in the next section.

Alloys containing 25 at.% and higher amounts of Ni, show a single recalescence event (Fig. 3(b)-3(d)). X-ray and SEM studies indicate the presence of primarily the C14 phase, and a small volume fraction of the α(Ti/Zr) phase for the alloys containing about 25 at. % Ni. For the $Ti_{40}Zr_{30}Ni_{30}$ alloy, pure C14 phase is observed, confirming primary nucleation of this phase directly from the undercooled liquid. The reduced undercooling for the Laves phase was found to be about 0.14, smaller than for the β(Ti/Zr) phase (0.18 on the average).

3.2 The primary nucleating phase in $Ti_{79-x}Zr_xNi_{21}$ alloys

The fact that the recalescence events for these alloys are inconsistent with the nucleation of either the C14 Laves or the β(Ti/Zr) phase, raises the possibility that the nucleating phase is metastable. If the first temperature rise is due to the nucleation and growth of a metastable phase, then the second thermal event could be associated with the subsequent decomposition of the metastable phase into the stable C14 Laves and the β(Ti/Zr) phases. The identification of such short-lived metastable phases is not easy, however. In-situ x-ray or neutron diffraction studies coupled with containerless processing and fast detectors, is the only direct method for the unambiguous identification of such metastable phases. The BESL facility has

331
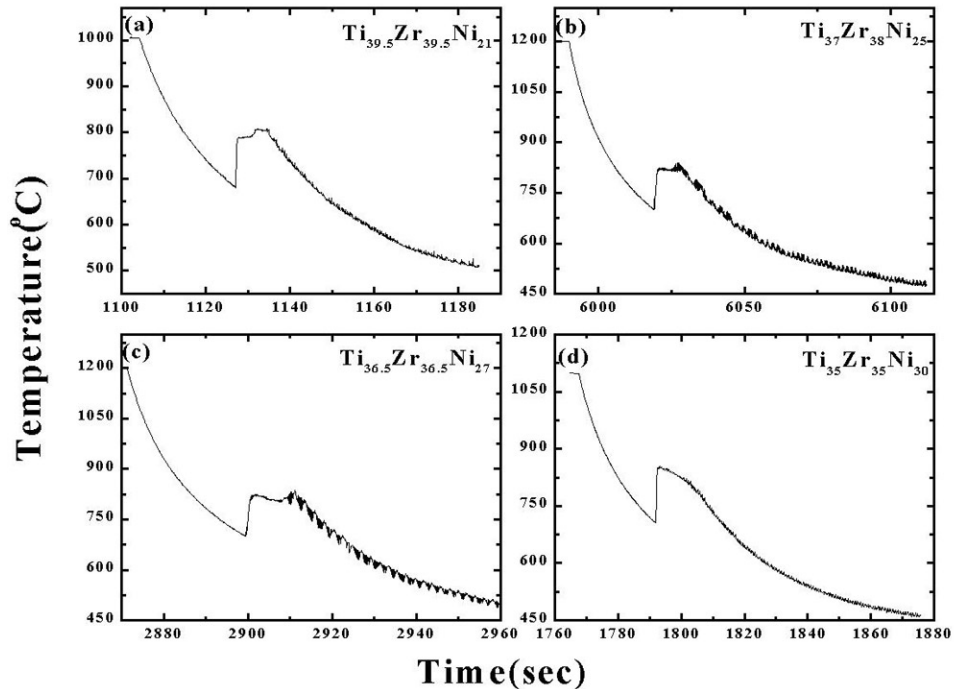
Fig. 3. Temperature-time cooling curves of undercooled Ti-Zr-Ni alloys.

been recently developed jointly by our group at Washington University, the NASA-ESL group led by J. Rogers, and representatives of MU-CAT at the Advanced Photon Source (APS), led by A. I. Goldman. This facility was recently used to study the structure and phase transitions of highly undercooled liquids of high temperature alloys using containerless processing techniques under high vacuum. The high flux synchrotron x-ray source, coupled with an image-plate detector, enabled BESL to acquire a complete set of diffraction data over a q-range from 0 to 8 Å^{-1} in less than one second. Fig. 4 shows the first results of in-situ x-ray diffraction studies on an electrostatically levitated liquid droplet. These were obtained from a $Ti_{39.5}Zr_{39.5}Ni_{21}$ alloy at 756 °C in the undercooled liquid state, during and after recalescence. The image plate was exposed typically for about 1 s to obtain each diffraction pattern.

These data clearly indicate that the liquid transforms to the i-phase during rcalescence, subsequently transforming to a phase mixture of the C14 Laves and the β(Ti/Zr) phases after recalescence, all within a few seconds. This is direct proof that the i-phase nucleates first from the undercooled liquid. The rise in temperature during recalescence drives its decomposition into the C14 Laves and the β(Ti/Zr) phases. The composition range over which the i-phase nucleates directly from the liquid is, however, restricted (20.5 at.% < Ni < 21.5 at.%, 29 at.% < Ti < 45 at.%). Our ground-based experiments, therefore, clearly identify three composition ranges in Ti-Zr-Ni alloys where the β(Ti/Zr), the Laves phase, and the i-phase are the primary nucleating phases from the undercooled liquid. The most important result is that ***the maximum reduced undercooling decreases from 0.18 (β(Ti/Zr)) to 0.14 (Laves) to 0.12 (i-phase) with increasing polytetrahedral order of the solid***. These results strongly support Frank's hypothesis and are in agreement with earlier electromagnetic levitation (EML) undercooling studies[12] on Al-based alloys. Quantitative studies are required, however, taking account of possible diffusion effects during nucleation [13] and using accurate measurements of the driving free energies and atomic mobilities.

332
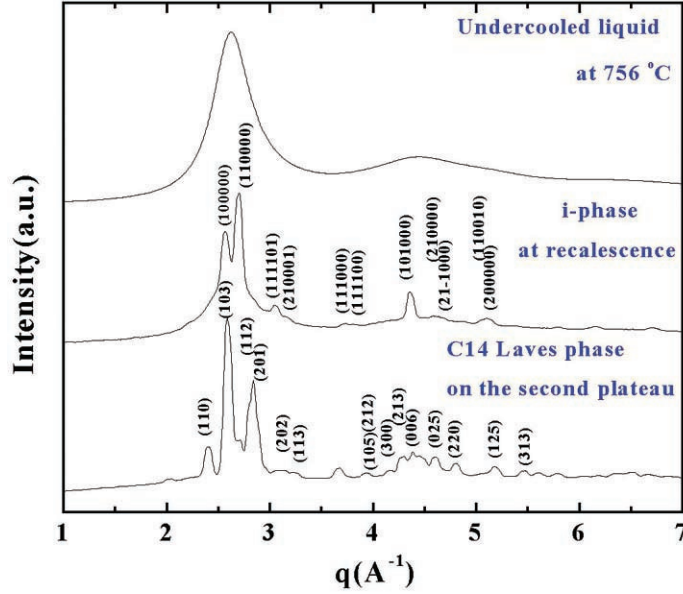
Fig. 4. In-situ x-ray diffraction showing the nucleation and growth of the i-phase and its subsequent decomposition to the C14 Laves phase during recalescence.

3.3 Liquid Specific Heat Measurements

A knowledge of the specific heat at constant pressure for the undercooled liquid, C_p^l, and the various solid phases is essential to the success of the proposed benchmark nucleation experiments on the ISS. An accurate analysis of the nucleation data requires that the driving free energy $\Delta G_v(T)$ be computed from the measured enthalpy of fusion at the melting temperature, ΔH_f, and the specific heat difference between the liquid and the solid phases, $\Delta C_p^{l,s} = C_p^l - C_p^s$,

$$\Delta G_v = \frac{\Delta H_f \, \Delta T}{T_m} - \int_{T_m}^{T} \Delta C_p^{l,s}(T')\, dT' + T \int_{T_m}^{T} \frac{\Delta C_p^{l,s}(T')}{T'}\, dT' \qquad (1)$$

where ΔT is the amount of undercooling (T_m - T). Unfortunately, few experimental data are available for ΔH_f and $\Delta C_p^{l,s}$, especially, for alloys and compounds with high melting temperatures. In the absence of experimental data, many workers have used approximate expression for $\Delta G_v(T)$[3]. However, no single expression is universally acceptable for different alloys. Further, the analysis of nucleation data with these approximate expressions often leads to orders of magnitude error in the estimated nucleation parameters[3, 14].

Because of the high vacuum and containerless processing capability, ESL is particularly suitable for specific heat measurements in the liquid and undercooled state for high temperature alloys, if the sample emissivity is known. In the ESL, the levitated sample cools freely by radiation loss. For a sample of radius, r, and emissivity, ε, the rate of heat loss at temperature T is given by the Stefan-Boltzmann relation,

$$H = 4\pi r^2 \sigma \varepsilon \left(T^4 - T_o^4\right), \qquad (2)$$

where k is the Stefan-Boltzmann constant, and T_o is the surrounding temperature. Balancing this heat loss with the cooling rate (dT/dt) for a sample of mass m, and specific heat C_p^l, one obtains

$$m C_p^l \left(\frac{dT}{dt}\right) = 4\pi r^2 \sigma \varepsilon \left(T^4 - T_o^4\right) \qquad (3)$$

333

By measuring the cooling for a sample of known radius, mass, and emissivity, the specific heat can be calculated from Eq. (3). Unfortunately, ε is known only for a few elements and alloys such as, Ni, Zr, and $Zr_{75}Ni_{25}$[15] over a limited spectral and temperature range. Therefore, ε was estimated either by extrapolating the data for $Zr_{75}Ni_{25}$ to the pyrometer wavelength used in the present investigation (1.2 – 1.4 μm), or by adjusting its value to match the known melting temperatures of binary alloys. Both methods gave $\varepsilon = 0.25$ for the Ti-Zr-Ni alloys for the wavelength range used. Any temperature dependence for ε was ignored, because it changes only by one to two percent between 1000 and 1500 K for pure Zr and a related binary $Zr_{75}Ni_{25}$ alloy[15].

The C_p^l for a large number of ternary Ti-Zr-Ni alloys in the liquid and undercooled state were determined from the free-cooling data. Fig. 5 shows the C_p^l data for a few representative compositions containing equal Ti and Zr and increasing Ni, which crystallize first into the β(Ti/Zr) phase. The most important trend is an increase in C_p^l as well as its temperature dependence with increasing Ni. In Fig. 6, the specific heat of Ti-Zr-Ni alloys containing higher Ni (21 at.% ≤ Ni ≤ 30 at.%) are shown. As pointed out in §3.2, the primary nucleating phase for the 21 at.% Ni alloy is the i-phase; it is the C14 Laves for the other compositions. The trend of an increase in C_p^l with increasing Ni is similar to that observed for the β(Ti/Zr) phase forming alloys. The important difference is that C_p^l goes through a maximum in the undercooled state. After careful consideration to all possible sources of error, we concluded that this is not an
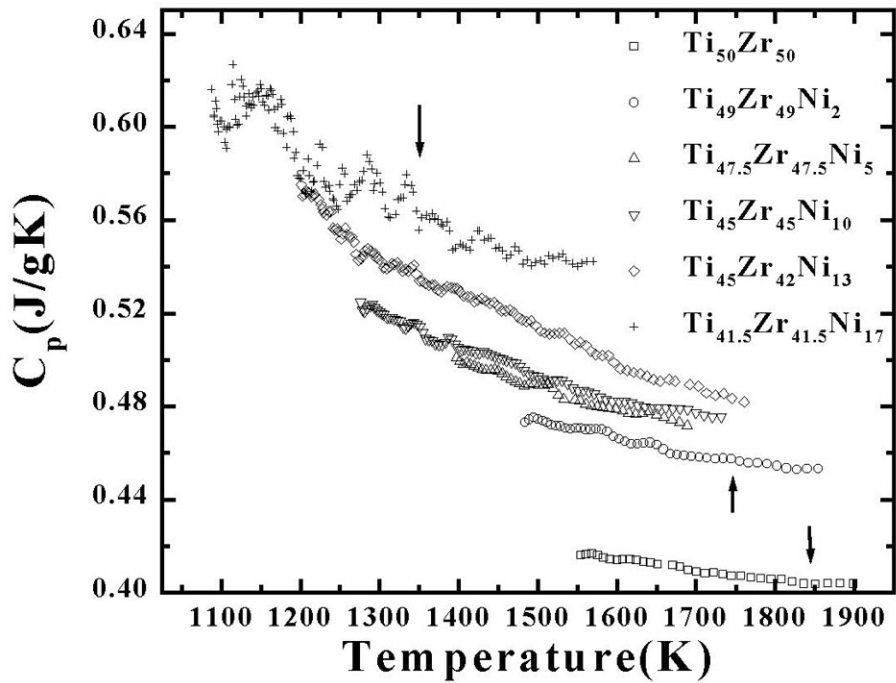
Fig. 5. Specific heat as a function of incresing Ni for alloys with equal concentration of Ti and Zr. Arrows indicate the liquidus temperatures.

experimental artifact. Further, no anomalous change in the liquid structures measured by BESL was observed in this temperature range that would suggest a phase separation in the undercooled liquid. Interestingly, Sommer found[16] that in ternary $Al_2La_3Ni_3$, C_p^l above T_g is smaller than at the liquidus temperature, although C_p^l increased with decreasing temperature, implying the existence of a maximum in C_p^l between T_g and the liquidus temperature. However, data in the intermediate temperature range

were not available to confirm this. This is the first known alloy system that shows a maximum in C_p^l. Sommer[16] tried to explain the possible maximum in C_p^l of $Al_{30}La_{50}Ni_{20}$ in terms of a competition between the chemical short-range order (CSRO) in the liquid binary alloy (Al_2Ni) and the CSRO in the ternary liquid phase ($Al_2La_3Ni_3$). To quantitatively apply this model to our data, more information on clusters present in the liquid is necessary. Qualitatively, however, the maximum in C_p^l should be related to a changing viscosity in the melt. The maximum should occur somewhere near T_g, where the viscosity rises rapidly. In contrast, the present maximum occurs around 0.05-$0.06T_m$. Interestingly, some recent molecular dynamics calculations[17] predicted a maximum in C_p^l, if the liquid changes its character from fragile to strong. Work is in progress to check this possibility in the present system. Also, modulated calorimetry measurements, possible in MSL-EML, are needed to confirm this peak in the specific heat.
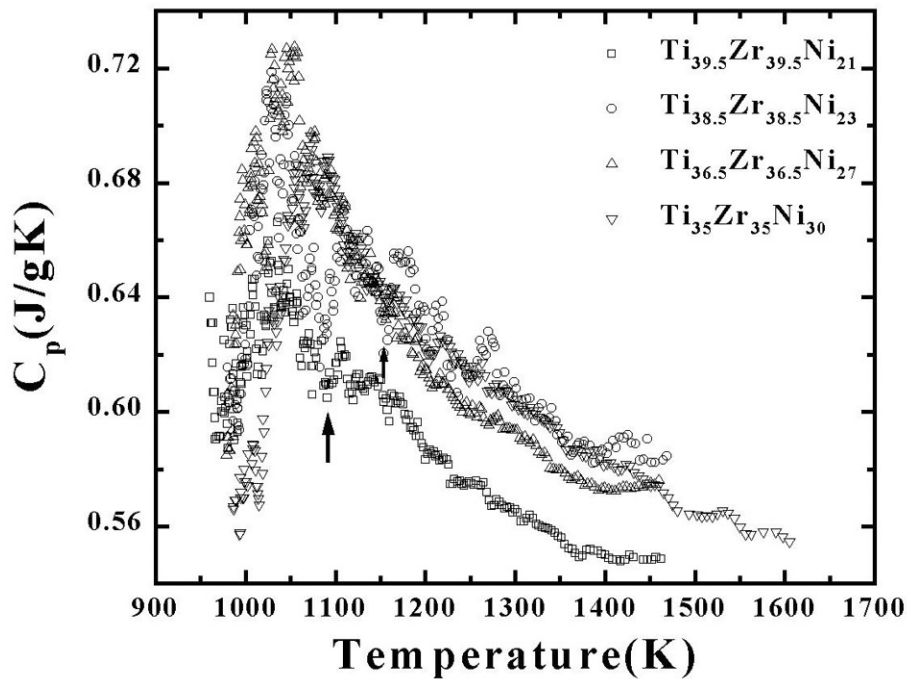
Fig. 6. Specific heat of Ti-Zr-Ni alloys containing higher Ni and equal Ti and Zr. Arrows indicate the liquidus temperatures of the corresponding compositions.

3.4 Viscosity and Surface Tension Measurements

A knowledge of the diffusion coefficient, D, in the undercooled liquid is essential for a detailed modeling of the nucleation of crystalline phases from the undercooled liquid[3]. In addition, viscosity can also provide important information on the short-range order of the undercooled liquid and show indications of a possible fragile to strong phase transition. Since the measurement of D is difficult and time consuming, especially for multi-component alloys where a knowledge of the diffusivity of each atomic species is preferred, D is, often, estimated from the viscosity (η) using the Stokes-Einstein relation ($D = kT/3\pi a\eta$, where k is the Boltzmann constant, T is the temperature, and the parameter a is of the order of the covalent radius). Although surface tension data are not necessary for nucleation studies, they are needed to estimate the surface-driven convection (Marangoni flow) during the droplet processing to assess the role of convective flow and diffusive flow on nonpolymorphic nucleation processes under terrestrial or microgravity conditions. The surface tension data are obtained naturally, if the viscosity is measured by the droplet oscillation technique.

The viscosity and surface tension of a liquid can be measured by observing the effects of induced oscillations in a droplet. If the radius, R, of a liquid drop undergoes surface oscillation of the form,

$$R = R_0(1+\delta \cos(\omega t)e^{-\lambda t}),\tag{4}$$

where δ is the amplitude, ω is the frequency, and λ is the damping constant of the oscillations, the frequency is related to the surface tension σ and the sample mass m by Rayleigh's formula,

$$\omega^2 = (32\pi\sigma)/(3m),\tag{5}$$

The damping constant λ is related to the viscosity η by Kelvin's formula,

$$\lambda = (20\pi\eta R_0)/(3m),\tag{6}$$

Measurement of the oscillation frequency, the damping constant, and the sample radius and mass can, therefore, be used to calculate the surface tension and viscosity of the liquid. Oscillations on a contamination- and distortion-free droplet are a necessary prerequisite for the success of this technique. This necessitates containerless processing (EML or ESL), preferably under microgravity[18, 19].

The viscosity of the i-phase forming composition $Ti_{37}Zr_{42}Ni_{21}$ was measured, both in the liquid and undercooled state before the onset of crystallization, using the ESL facility at MSFC, Huntsville. The viscosity data are shown in a semi-logarithmic plot in Fig. 7. The activation energy calculated from the slope of the straight line is 61 KJ/mol. This value is much higher than in transition metals (50.2 KJ/mol for Ni and 41.4 KJ/mol for Fe[20]), suggesting the formation of a network of clusters in the liquid. The
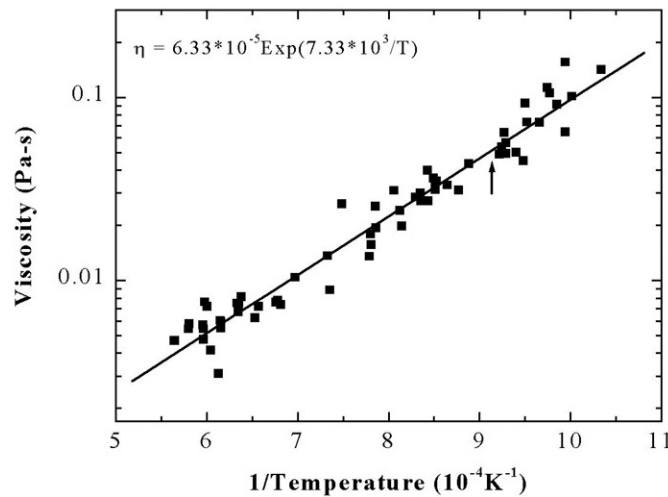
Fig. 7. Semi-logarithmic plot of the temperature dependence of viscosity of $Ti_{37}Zr_{42}Ni_{21}$ alloy in the liquid and undercooled state.

smooth extrapolation of the data from the liquid to the undercooled state, however, shows no abrupt change in the short-range order of the liquid below the liquidus temperature (marked by an arrow). Interestingly, this is the first measurement of viscosity of any Ti-Zr-Ni alloy in the liquid and undercooled state. Measurements of other compositions which nucleate β(Ti/Zr) (low Ni) and the C14 Laves phase (27 at.% < Ni < 33 at.%) are in progress.

336

4. Conclusions

From extensive ground based work on the phase diagram and undercooling studies of Ti-Zr-Ni alloys, we have clearly identified the composition of three different phases with progressively increasing polytetrahedral order such as, β(Ti/Zr), the C14 Laves phase, and the i-phase, that nucleate directly from the undercooled liquid. The reduced undercooling decreases progressively with increasing polytetrahedral order in the solid, supporting Frank's hypothesis[4]. A new facility for direct measurements of the structures and phase transitions in undercooled liquids (BESL) was developed and has provided direct proof of the primary nucleation of a metastable icosahedral phase in some Ti-Zr-Ni alloys. The first measurements of specific heat and viscosity in the undercooled liquid of this alloy system have been completed. Other than the importance of thermo-physical properties for modeling nucleation and growth processes in these materials, these studies have also revealed some interesting new results (such as a maximum of C_p^l in the undercooled state). These ground-based results have clearly established the necessary background and the need for conducting *benchmark* nucleation experiments at the ISS on this alloy system.

References

1. Fahrenheit, D.B., *Phil. Trans. Royal Soc.*, 1724, **39,** p. 78.
2. Turnbull, D., *J. Chem. Phys.* 1952, **20**(3), p. 411.
3. Kelton, K.F., in *Solid State Physics*, H. Ehrenreich and D. Turnbull, Editors. 1991, Academic Press, Boston, p. 75.
4. Frank, F.C., *Proc. Royal Soc.*, 1952, **215A,** p. 43.
5. Echt, O., K. Sattler, and E. Recknagel, *Phys. Rev. Lett.*, 1981, **47,** p. 1121.
6. Mühlbach, J., et al., *Phys. Rev. Lett.*, 1982, **87A,** p. 415.
7. Schechtman, D., et al., *Phys. Rev. Lett.*, 1984, **53,** p. 1951.
8. Holzer, J.C. and K.F. Kelton, *Acta Metal. Mater.*, 1991, **39**(8), p. 1833.
9. Stroud, R.M., *Ph. D. Thesis* 1996, Washington University, St. Louis, p. 139.
10. Lee, G.-W., et al., *Phil. Mag. Lett.*, 2002, **82,** p. 199.
11. Nelson, D.R. and F. Spaepen, in *Solid State Phys.*, D. Turnbull, Editor. 1989, Academic, Boston, p. 1.
12. Holland-Moritz, D., et al., *Acta Mater.*, 1998, **46**(5), p. 1601.
13. Kelton, K.F., *Acta Mater.*, 2000, **48,** p. 1967.
14. Perepezko, J.H., *J. Non-Crystalline Solids*, 1993, **156-158,** p. 463.
15. Krishnan, S. and P.C. Nordine, *J. Appl. Phys.*, 1996, **80**(3), p. 1735.
16. Sommer, F., *Mat. Sci. and Eng.*, 1997, **A226-228,** p. 757.
17. Saika-Volvod, I., P.H. Poole, and F. Sciortino, *Nature*, 2001, **412,** p. 514.
18. Egry, I., et al., *Science Laboratory (MSL-1) Final Report*. 1998. Huntsville, Alabama: NASA.
19. Fuji, H., T. Matsumoto, and K. Nogi, *Acta Mater.*, 2000, **48,** p. 2933.
20. Brandes, E.A. and G.B. Brook, *Smithells Metals Reference Book*. Seventh ed, ed. E.A. Brandes and G.B. Brook. 1992, Oxford: Butterworth-Heinemann.